Science of the Total Environment 932 (2024) 172996

Contents lists available at ScienceDirect

Science of the Total Environment

journal homepage: www.elsevier.com/locate/scitotenv

Anaerobic biodegradation of perfluorooctane sulfonate (PFOS) and microbial community composition in soil amended with a dechlorinating culture and chlorinated solvents

Michelle M. Lorah [a,*], Ke He [b], Lee Blaney [b], Denise M. Akob [c], Cassandra Harris [c,1], Andrea Tokranov [d], Zachary Hopkins [e], Brian P. Shedd [f]

[a] U.S. Geological Survey, Maryland-Delaware-D.C. Water Science Center, Baltimore, MD 21228, USA
[b] University of Maryland Baltimore County, Department of Chemical, Biochemical, and Environmental Engineering, Baltimore, MD 21250, USA
[c] U.S. Geological Survey, Geology, Energy, & Minerals Science Center, Reston, VA 20192, USA
[d] U.S. Geological Survey, New England Water Science Center, Pembroke, NH 03275, USA
[e] U.S. Geological Survey, Eastern Ecological Science Center, Kearneysville, WV 25430, USA
[f] U.S. Army Corps of Engineers, U.S. DOD Environmental Programs Branch, Environmental Division, Headquarters, Washington, D.C. 20314, USA

HIGHLIGHTS

- PFOS biodegradation occurred in soil microcosms with added dehalogenating culture.
- Initial presence of chlorinated volatile organic compounds enhanced PFOS removal.
- Shorter chain perfluorinated sulfonates were minor PFOS metabolites.
- Increased abundance of sulfate reducers was associated with PFOS removal.
- Further research for a PFAS *in situ* bioremediation method is warranted.

GRAPHICAL ABSTRACT

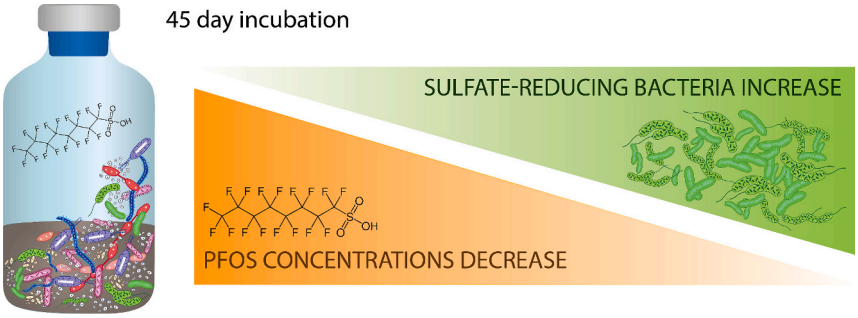

ARTICLE INFO

Editor: Jay Gan

Keywords:
PFAS biodegradation
Perfluorinated sulfonate
PFAS contaminated soil
Dehalogenating culture
Sulfate reducers
Chlorinated volatile organic compounds

ABSTRACT

Perfluorooctane sulfonate (PFOS), one of the most frequently detected *per-* and polyfluoroalkyl substances (PFAS) occurring in soil, surface water, and groundwater near sites contaminated with aqueous film-forming foam (AFFF), has proven to be recalcitrant to many destructive remedies, including chemical oxidation. We investigated the potential to utilize microbially mediated reduction (bioreduction) to degrade PFOS and other PFAS through addition of a known dehalogenating culture, WBC-2, to soil obtained from an AFFF-contaminated site. A substantial decrease in total mass of PFOS (soil and water) was observed in microcosms amended with WBC-2 and chlorinated volatile organic compound (cVOC) co-contaminants — 46.4 ± 11.0 % removal of PFOS over the 45-day experiment. In contrast, perfluorooctanoate (PFOA) and 6:2 fluorotelomer sulfonate (6:2 FTS) concentrations did not decrease in the same microcosms. The low or non-detectable concentrations of potential metabolites in full PFAS analyses, including after application of the total oxidizable precursor assay, indicated

* Corresponding author.
E-mail address: mmlorah@usgs.gov (M.M. Lorah).
[1] Present address: U.S. Environmental Protection Agency, Office of Pesticide Programs, Environmental Fate and Effects Division, Washington, D.C., 20460, USA.

https://doi.org/10.1016/j.scitotenv.2024.172996
Received 21 February 2024; Received in revised form 29 April 2024; Accepted 2 May 2024
Available online 6 May 2024

that defluorination occurred to non-fluorinated compounds or ultrashort-chain PFAS. Nevertheless, additional research on the metabolites and degradation pathways is needed. Population abundances of known dehalorespirers did not change with PFOS removal during the experiment, making their association with PFOS removal unclear. An increased abundance of sulfate reducers in the genus *Desulfosporosinus* (Firmicutes) and *Sulfurospirillum* (Campilobacterota) was observed with PFOS removal, most likely linked to initiation of biodegradation by desulfonation. These results have important implications for development of *in situ* bioremediation methods for PFAS and advancing knowledge of natural attenuation processes.

Abbreviations

AFFF	aqueous film forming foam
cVOC	chlorinated volatile organic compound
12DCA	1,2-dichloroethane
12DCE	cis- and trans-1,2-dichloroethylene
OTU	operational taxonomic unit
PFAA	perfluoroalkyl acid
PFAS	per- and polyfluoroalkyl substances
PFBA	perfluorobutanoate
PFBS	perfluorobutane sulfonate
PFHxS	perfluorohexane sulfonate
PFOA	perfluorooctanoate
PFOS	perfluorooctane sulfonate
B-PFOS	branched isomers of PFOS
L-PFOS	linear isomers of PFOS
PFPeS	perfluoropentane sulfonate
6:2 FTS	6:2 fluorotelomer sulfonate
112TCA	1,1,2-trichloroethane
TCE	trichloroethylene
TeCA	1,1,2,2-tetrachloroethane
TOP	total oxidizable precursor
VC	vinyl chloride

1. Introduction

Per- and polyfluoroalkyl substances (PFAS) are widespread contaminants of emerging concern owing to the use of aqueous film-forming foams (AFFF) for firefighting at airports and military bases and the use of PFAS in a multitude of other consumer and industrial products and applications (Anderson et al., 2016; Glüge et al., 2020). Research over the past 20 years has provided increased evidence of the adverse effects of PFAS on human health (Rogers et al., 2021; Sunderland et al., 2019) and ecosystems (Ankley et al., 2021). In 2024, the U.S. Environmental Protection Agency (USEPA) established drinking water regulations for five individual PFAS, including perfluorooctane sulfonate (PFOS) and perfluorooctanoate (PFOA) (USEPA, 2024). Maximum contaminant level goals of 0 nanograms per liter (ng/L) were set for PFOS and PFOA as likely carcinogens, and maximum contaminant levels of 4 ng/L were set for each compound in this final rule (USEPA, 2024).

PFOS and PFOA are the most commonly reported PFAS, and PFOS concentrations in soil and groundwater are often significantly higher than PFOA levels (Johnson et al., 2022). PFOS is a major component and PFOA a minor byproduct of legacy AFFF produced by electrochemical fluorination, which was the dominant production process through the 1990s (Weber et al., 2017; Schaefer et al., 2018). Amid concerns of the persistence, bioaccumulation, and toxicity of PFOS and PFOA, fluorotelomerization became the primary method for PFAS production in the 2000s to replace PFOS-based electrochemical fluorination. While legacy fluorotelomer-based AFFF contained long-chain polyfluorinated precursors that could be transformed to PFOA (Harding-Marjanovic et al., 2015), more recent formulations primarily shifted towards C6 short-chain length PFAS, such as 6:2 fluorotelomer sulfonate (6:2 FTS) (Buck et al., 2011; Wang et al., 2015).

Interest in microbially mediated transformation reactions is driven by the need to understand the fate of complex PFAS mixtures after their release from source areas and to develop effective remediation and monitored natural attenuation methods for the wide range of PFAS compounds and concentrations (Newell et al., 2021b, 2021a). To date, much of the research has focused on precursor biotransformation through oxidative processes under aerobic conditions, which primarily results in transformation to apparently stable and mobile perfluoroalkyl acid (PFAA) end products (Zhang et al., 2021; Sharifan et al., 2021; Harding-Marjanovic et al., 2015). Although understanding precursor transformations is critical to defining the transport and risk of PFAS contamination in the environment, biodegradation of PFAAs is the ultimate goal for PFAS mitigation through bioremediation. Evidence of biodegradation (or mineralization) under aerobic or anaerobic conditions is highly limited for PFAAs (Ochoa-Herrera et al., 2016; Park et al., 2017; Sharifan et al., 2021). Reductive defluorination of PFAS can theoretically yield substantial energy to microbes (Bossert et al., 2003; Parsons et al., 2008), but little evidence of microbial degradation of perfluorinated compounds under anaerobic conditions existed prior to studies by Huang and Jaffé (2019) and Yu et al. (2020). Huang and Jaffé (2019) reported the first comprehensive study of PFOA and PFOS bioreductive defluorination using pure and enrichment cultures of *Acidimicrobium sp.* strain A6 (A6) (Huang et al., 2016; Huang and Jaffé, 2018; Huang and Jaffé, 2019). Production of fluoride, acetate, and short chain perfluorinated compounds occurred during anaerobic degradation of PFOS and PFOA by A6 (Huang and Jaffé, 2019; Huang et al., 2022).

Yu et al. (2020) reported anaerobic biodegradation by reductive defluorination for two unsaturated (carbon double bond) C6 carboxylic acids, one polyfluorinated and one perfluorinated, using the dehalogenating culture KB-1. Formation of defluorinated transformation products and fluoride release were observed when lactate was supplied as an electron donor and the PFAS was the sole electron acceptor (Yu et al., 2020). However, biodefluorination was not observed for saturated PFAS, including PFOA, in this study or a follow-on investigation with 13 other fluorinated carboxylic acids (Yu et al., 2022). Reductive dehalogenating species or the reductive dehalogenase enzymes in the KB-1 culture did not appear to be linked to microbial degradation of the unsaturated PFAS, but degradation was only observed in the presence of live cultures (Yu et al., 2020).

Additional research on anaerobic microbial reductive biodegradation of PFAS under *in situ* conditions is important due to the prevalence of anoxic conditions in subsurface plumes and groundwater discharge areas (Parsons et al., 2008; Kucharzyk et al., 2017). To investigate PFAS biotransformation and potential bioremediation applications using reductive degradation processes, we conducted laboratory experiments to determine if the presence of chlorinated volatile organic compound (cVOC) co-contaminants and known dehalorespirers could stimulate transformation of PFOS and other PFAS through reductive defluorination. We conducted anaerobic experiments with the previously established, diverse dehalogenating culture, WBC-2 (Jones et al., 2006; Lorah

et al., 2008), as well as native microorganisms from contaminated soils. WBC-2 was developed to degrade both saturated cVOCs, particularly 1,1,2,2-tetrachloroethane (TeCA), and unsaturated cVOCs, including trichloroethylene (TCE) and its daughter products (Lorah et al., 2008; Jones et al., 2006). Our objectives were to (1) determine if PFAS can be biodegraded under anoxic conditions and (2) add to the limited available data on microbial populations associated with PFAS degradation, including the potential role of dehalogenating and sulfate-reducing microbes. PFOS was selected as a primary perfluorinated compound because of its prevalence in legacy AFFF and negligible removal by oxidation-based treatment processes (Schaefer et al., 2018; Park et al., 2016). Two additional compounds, 6:2 FTS and PFOA, were included in these experiments to identify the impacts, respectively, of a polyfluoroalkyl moiety adjacent to the sulfonate head group and of a perfluorinated carboxylate with comparable carbon chain length as PFOS, respectively, on biodegradation.

2. Materials and methods

2.1. Microcosm preparation and sampling

Laboratory tests are summarized here, and the accompanying data release contains all experimental data (Lorah et al., 2024). Microcosms were prepared with soil obtained near a former fire-fighting training area at a military installation (Fort Drum, New York, USA) known to contain relatively low PFAS levels. Soil (fine/silty sand) was collected from a depth of 2.5 to 8.5 cm below land surface and transported to the laboratory on ice. Soil was passed through a 2-mm sieve in an anaerobic glove chamber and thoroughly mixed before use in experiments.

Simulated groundwater was used to prepare a slurry with a water-to-soil ratio of 2:1 for the microcosms (Lorah et al., 2024). The simulated groundwater had a pH of 7.0 and contained 8.5 mg/L KH_2PO_4, 22 mg/L K_2HPO_4, 33 mg/L Na_2HPO_4, 10 mg/L $Ca_3(PO_4)_2$, 1.25 mg/L $FeCl_3{\cdot}6H_2O$, 100 mg/L $(NH_4)_2SO_4$, and 25 mg/L $MgSO_4{\cdot}7H_2O$. Microcosms (Table S1 and Table 1) were constructed in an anaerobic chamber and in 164-mL glass serum bottles closed with crimped butyl stoppers for sacrificial sampling at each time point. Microcosms were incubated for 45 days in an anaerobic chamber at room temperature (22–23 °C). All microcosm treatments were prepared in duplicate and sacrificed for sampling at each time point (days 0, 24, and 45).

The microcosms were amended to nominal aqueous-phase concentrations of 100 μg/L (0.20 μmol/L) PFOS, 50 μg/L (0.12 μmol/L) PFOA, and 50 μg/L (0.12 μmol/L) 6:2 FTS at the beginning of the experiment (day 0). Treatments were prepared with and without bioaugmentation with the WBC-2 dehalogenating culture (3.3 % *v*/v). Two PFAS-amended treatments were bioaugmented with WBC-2 — treatment WSEDT that also contained added cVOCs and treatment WSED that did not have added cVOCs (Table 1). WBC-2 was obtained from SiREM Lab (Guelph, Ontario, Canada). For the cVOC-amended treatments, microcosms were only spiked at day 0, with nominal aqueous-phase concentrations of 1000 μg/L (6.0 μmol/L) TeCA and 100 μg/L (0.76 μmol/L) TCE.

Two microcosm treatments were prepared without WBC-2, namely treatment SEDT amended with PFAS and cVOCs and a live control (LC) treatment. The LC treatment was unamended to provide a control for changes in the native microbial community due to incubation bottle effects. Sodium lactate was added to give 5 mM lactate to all soil microcosm treatments, except the LC treatment, as an electron donor to support reductive dehalogenation. A deionized water (DI) control without soil also was prepared with the PFAS and cVOCs to evaluate the amendment concentrations and potential abiotic losses over time that could be due to processes other than soil sorption, such as volatile losses or sorption to the bottle.

Table 1
Summary of microcosm treatments. Treatments contained soil mixed with simulated groundwater (1:2 ratio by volume), except treatment DI which did not contain soil.

Treatment	Soil	Lactate	WBC-2	cVOCs	PFAS
WSEDT	+	+	+	+	+
SEDT	+	+	−	+	+
WSED	+	+	+	−	+
LC	+	−	−	−	−
DI	−	−	−	+	+

2.2. Amended PFAS and cVOC analysis

The microcosm slurries were centrifuged to obtain water and soil samples from each microcosm bottle for analysis of PFOS, PFOA, and 6:2 FTS. Select microcosm water samples also were analyzed for a wider suite of 41 PFAS as described in Section 2.3. Detailed preparation and analytical protocols for PFOS, PFOA, and 6:2 FTS are described in the supplemental information (Text S1, Table S2, Fig. S1). Triplicate analyses were performed for each sample, and the mean concentration ± standard deviation was reported (Lorah et al., 2024). For the water samples from the microcosms, the linear (L-PFOS) isomers of PFOS were quantified using an L-PFOS analytical standard, and the branched (B-PFOS) isomers were determined using the integrated peak area for B-PFOS with the calibration for L-PFOS. Standards were obtained to quantify both L-PFOS and B-PFOS in the soil samples; in particular, an L-PFOS standard (Wellington Laboratories, Guelph, Ontario, Canada) and a mixed standard containing both L-PFOS and B-PFOS (Sigma-Aldrich) were used to generate separate L-PFOS and B-PFOS calibrations. For quality assurance, water samples from the DI treatment were rerun to quantify the aqueous-phase L-PFOS and B-PFOS concentrations (Table S3). The average L-PFOS concentration in the water was 2.5 times greater than the B-PFOS content, in agreement with the composition of the standard that was used to amend the microcosms with PFOS.

The analytical standards of PFOS, PFOA, 6:2 FTS, and their mass-labeled analogs, namely sodium perfluoro-1-[1,2,3,4-13C_4]octane sulfonate (MPFOS), perfluoro-n-[1,2,3,4-13C4]octanoic acid (MPFOA), sodium 1H,1H,2H,2H-perfluoro-[1,2-13C_2]octane sulfonate (M2-6:2 FTS), perfluoro-n-[$^{13}C_8$] octanoic acid (M8PFOA), and sodium perfluoro-1-[$^{13}C_8$] octane sulfonate (M8PFOS), were purchased from Wellington Laboratories (Guelph, Ontario, Canada). MPFOA, M2-6:2 FTS, and MPFOS were used as internal standards to correct matrix effects during LC-MS/MS analysis, and M8PFOA and M8PFOS were used as surrogates to track analyte recovery during the extraction and cleanup processes.

Replicate water and soil samples were collected for cVOC analysis from at least one of the duplicate microcosm bottles in a treatment set at each time step and analyzed by gas chromatography mass spectrometry, using a modified version of USEPA Method 542 (Majcher et al., 2007). Replicates were analyzed for 25 % of the samples collected, and the average relative percent difference was 7.80 % for detected constituents. Water samples (2 mL) were collected for methane analysis by gas chromatography with a flame ionization detector, using previously reported methods (Majcher et al., 2007; Lorah et al., 2022), to evaluate redox conditions for selected microcosm bottles.

2.3. PFAS mass balance and comprehensive PFAS analysis

The concentrations of the amended compounds PFOS, PFOA, and 6:2 FTS analyzed in the microcosm water and soil samples at each time point were converted to mass using the volume of water and mass of soil in each bottle, respectively (Table S1). The change in total mass of each PFAS (*i.e.*, sum of PFAS mass in the water and soil) was determined over the experiment duration. The total mass was normalized using the initial mass measured at day 0 for each compound to compare changes among treatments.

A full suite of 41 target PFAS was analyzed for select water samples

from treatments WSED and SEDT using two dilutions to achieve low detection levels for PFAS. The full PFAS analysis was done at the U.S. Geological Survey (USGS) with a direct injection isotope dilution method on an Orbitrap Exploris 120 liquid chromatograph with high resolution mass spectrometry, as described in Lorah et al. (2024). The detected concentrations and the sum of PFAS on molar and fluorine equivalent bases (Text S2 and Table S4) are summarized in Table S6 for these full PFAS analyses. The same select water samples from treatments WSED and SEDT were subjected to the total oxidizable precursor (TOP) assay to assess possible production of polyfluoroalkyl metabolites in the microcosms that could not be detected by the standard full suite analysis (Text S2). Differences in PFAS concentrations before and after the TOP assay are summarized in Tables S6 and S7. However, these calculations utilized post-TOP concentrations with exceedances of the highest calibration point and, thus, the TOP assay results were primarily employed to determine the presence or absence of unknown metabolites in the two treatments.

2.4. Microbial community analyses

Microcosm slurry samples were collected for microbial community analysis after collection of liquid required for chemical analyses. Microbial communities at each sampling point were characterized using Illumina 16S rRNA gene iTag sequencing through the USGS Reston Microbiology Laboratory according to methods described in Mumford et al. (2020). In brief, DNA was extracted from the samples using the DNeasy PowerSoil kit (Qiagen, Inc., Hilden, Germany) according to the manufacturer's protocols. Extracted DNA was quantified using the Quant-iT double-stranded DNA (dsDNA) High Sensitivity assay kit (Life Technologies, Carlsbad, CA) according to the manufacturer's instructions. Genomic DNA was diluted to a final concentration of 10 ng/μL using nuclease-free water (Ambion, Inc., Austin, TX) then shipped to Michigan State University's Research Technology Support Facility (RTSF, East Lansing, MI) for Illumina 16S iTag sequencing.

Amplicon libraries of the V4 hypervariable region of the 16S rRNA gene were prepared using dual indexed, Illumina compatible primers 515f and 806r (Caporaso et al., 2012; Apprill et al., 2015; Parada et al., 2016; Walters et al., 2016) following the protocols developed by the Patrick Schloss laboratory (Kozich et al., 2013). Following polymerase chain reaction (PCR), all products were batch normalized using Invitrogen SequalPrep DNA Normalization (Invitrogen, Carlsbad, CA) plates, and products were recovered from the plate and pooled. The pool was quality controlled and quantified using a combination of Qubit dsDNA HS, Agilent 4200 TapeStation HS DNA1000, and Invitrogen Collibri Library Quantification qPCR assays. This pool was loaded onto an Illumina MiSeq Standard v2 flow cell, and sequencing was performed in a 2 × 250 base pair (bp) paired-end format using a 500-cycle v2 reagent cartridge. Custom sequencing primers were added to appropriate wells of the reagent cartridge as described in Kozich et al. (2013). Base calling was done by Illumina Real-Time Analysis (RTA) v1.18.54, and the RTA output was demultiplexed and converted to FastQ format with Illumina Bcl2fastq v2.20.0.

Initial quality control, alignment, and taxonomic assignment of microbial sequence data were performed using mothur v1.43.0 according to the mothur MiSeq standard operating procedure (Schloss et al., 2009; Kozich et al., 2013; Schloss, 2021) and using the USGS Advanced Research Computing Yeti high-performance computing facility. Operational taxonomic units (OTUs) were generated based on a 97 % similarity cutoff against the Silva 138 non-redundant database (Quast et al., 2013; Yilmaz et al., 2014). Statistical and diversity analyses were performed in R (R Core Team, 2015) using CORE components and the VEGAN, PHYLOSEQ, and DESeq2 packages (McMurdie and Holmes, 2013; R Core Team, 2015; Oksanen et al., 2018; Oksanen et al., 2019; Love et al., 2014); and Prism version 9 (GraphPad Software, San Diego, CA) as described in the Supplemental Information. All mothur and R codes are provided in the Supplemental Information. Two samples that had <5000 reads, "LC Day 24.1_2" and "SEDT Day0.1_2," were removed for the non-metric multidimensional scaling (NMDS) analysis but retained for other analyses as only duplicates were available. Sequences are available from the NCBI Sequence Read Archive under BioProject PRJNA938174 and BioSample accession numbers SAMN33427333 through SAMN33427372, and taxonomic assignment for all OTUs is available as a biom file in Lorah et al. (2024).

3. Results and discussion

3.1. PFOS concentrations and mass removal rates

Aqueous-phase PFOS concentrations substantially declined from day 0 to day 45 in the soil slurry microcosm treatments amended with PFAS and cVOCs, including the bioaugmented treatment WSEDT and the non-bioaugmented treatment SEDT (Fig. 1A). In contrast, aqueous-phase PFOS concentrations in treatment WSED, which was bioaugmented with WBC-2 but not amended with cVOCs, decreased from day 0 to day 24 and then plateaued between days 24 and 45. Sorption to the soil partly accounted for the decrease in aqueous-phase PFOS concentrations in treatment WSEDT from day 24 to day 45, because PFOS levels in the soil increased during this period (Fig. 1B). However, mass balances of total PFOS in the microcosms indicate that sorption or other abiotic processes could not fully account for the decrease in PFOS mass in SEDT and WSEDT (Fig. 2 and Table 2). In the three soil treatments with added PFAS, about 20 % of the total mass PFOS was distributed in the soil on

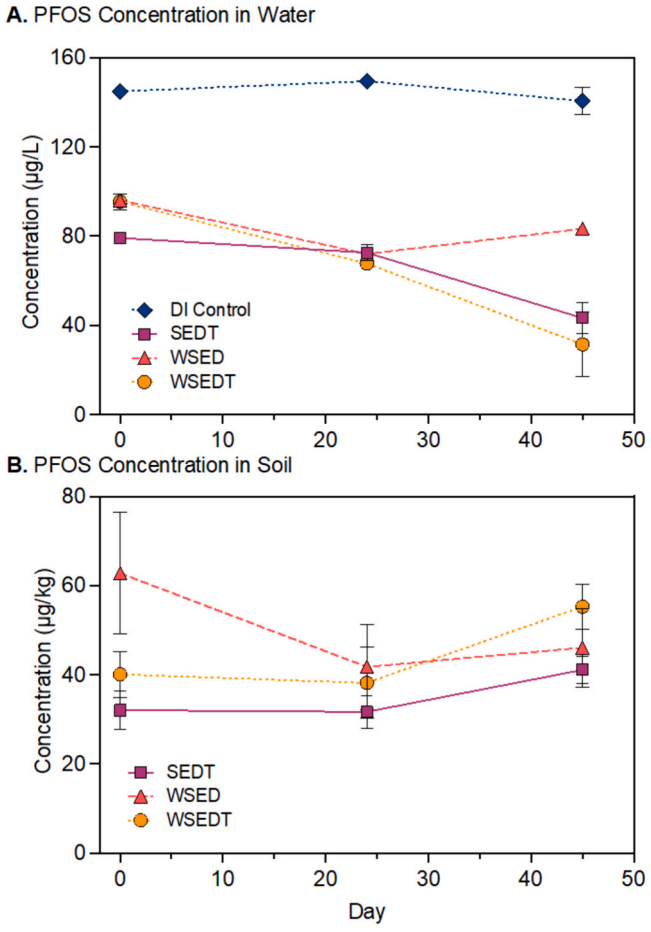

Fig. 1. Concentrations of PFOS (sum of linear and branched isomers) in microcosm (A) water and (B) soil samples. The reported concentrations are the mean of triplicate analyses of samples collected from duplicate microcosm bottles for each treatment. Error bars show standard deviation of mean values for duplicate microcosms.

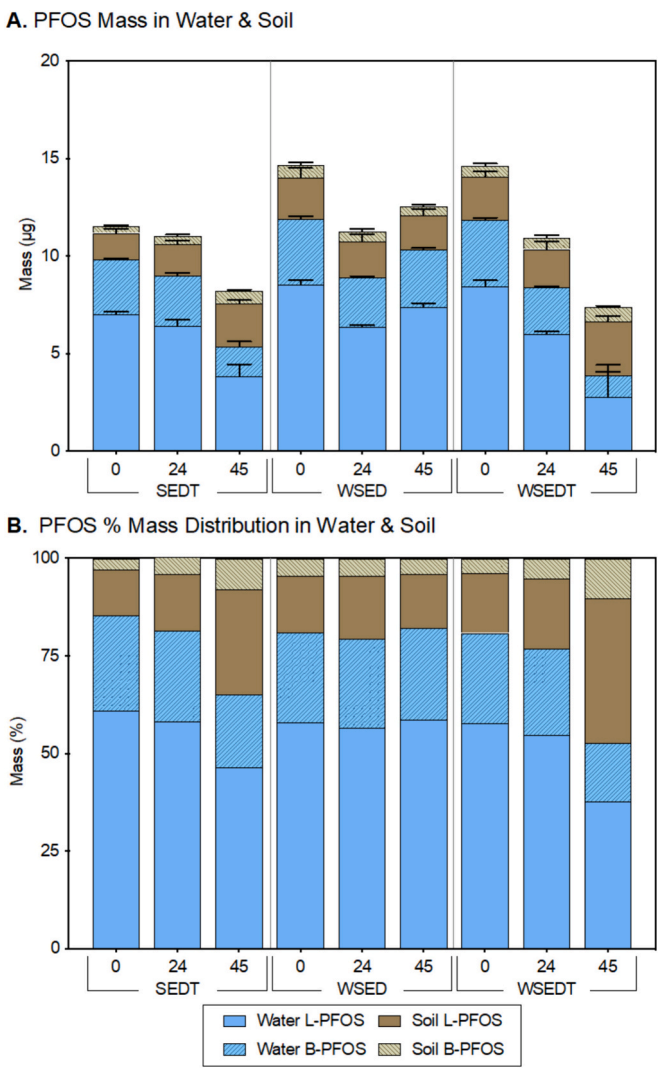

Fig. 2. PFOS in microcosms shown as (A) mass and (B) percent mass distribution of L-PFOS and B-PFOS in water and soil samples for each time step indicated in days. Error bars show standard deviation of mean values for duplicate microcosms.

day 0, which included 2–4 % as B-PFOS and 16–18 % as L-PFOS (Fig. 2). The unamended LC treatment had PFOS concentrations that were below detection in all water (< 0.5 µg/L) and soil (<0.5 µg/kg) samples (data available in Lorah et al., 2024).

The percent removal of total PFOS mass in the WSEDT treatment was substantially greater than observed in the other treatments and for 6:2 FTS and PFOA (Table 2 and Fig. 3A). Total mass removal of PFOS in the WSEDT treatment, which included the WBC-2 dehalogenating culture and cVOCs, was 46.4 ± 11.0 % over the 45-day experiment. The SEDT treatment with added cVOCs but no WBC-2 culture also had a significant, but lower, PFOS removal of 25.5 ± 6.6 % (Table 2). The first-order rate constants for PFOS mass removal were 0.0159 ± 0.0052 and 0.0075 ± 0.0021 d^{-1} in the WSEDT and SEDT microcosms, respectively, with corresponding half-lives of 48.8 ± 16.0 and 100.6 ± 28.0 d, respectively (Table 2). In contrast, the WSED treatment, which was amended with WBC-2 but not cVOCs, only had 11.5 ± 0.9 % mass removal of PFOS over the 45-day experiment. Although the initial PFOS mass removal in WSED (day 0 to 24) was approximately equal to the removal observed in the WSEDT treatment (Fig. 3A), PFOS concentrations did not continue to decrease in WSED after day 24, yielding an overall first-order rate constant of 0.0036 ± 0.00022 d^{-1} (Table 2). cVOC degradation and microbial community composition in the treatments assisted in evaluating the differences in PFOS removal, as discussed in Sections 3.4 and 3.5, respectively.

Higher concentrations (Fig. S2) and mass (Fig. 2) of L-PFOS were observed in the soil compared to B-PFOS, as expected due to the greater proportion of L-PFOS in the PFOS solution used to amend the microcosms. The masses of L-PFOS and B-PFOS that were measured in the soil samples were linearly correlated ($r^2 = 0.82$), indicating that sorption did not greatly differ between the two isomers for these test conditions (Fig. S3). Bio-uptake, which includes contaminant partitioning into phospholipid layers of cell membranes and incorporation into biofilm matrices of extracellular polymeric substances, has been measured for PFOS in laboratory and field studies (Fitzgerald et al., 2018; Munoz et al., 2018). Amendment of WBC-2 did not seem to affect sorption, however, because the change in PFOS soil mass in the treatments with (WSEDT) and without (SEDT) added culture was not significant (Mann-Whitney $U = 8.0$, $p = 0.05$) (Fig. 2B). Formation of iron complexes has been identified as a factor that potentially affects aqueous-phase PFOS concentrations at acidic pH (Park et al., 2018), but the solution pH was >7.0 in our experiment (Table S1).

3.2. PFOA and 6:2 FTS concentrations and mass removal

In contrast to the high PFOS mass removal in WSEDT and SEDT, no consistent concentration (Figs. S3 and S4) or mass removal (Fig. 3B and C) trends were identified for PFOA or 6:2 FTS. The highest PFOA percent removal was 11.0 ± 10.0 % in treatment WSEDT (Table 2). The change in 6:2 FTS total mass was only about 2 % in the WSEDT and WSED treatments (Table 2). The greatest mass change for 6:2 FTS was observed in treatment SEDT, which was amended with cVOCs but not the WBC-2 culture — a 19.1 ± 1.4 % increase in mass was calculated from day 0 to day 45. However, the apparent increase in 6:2 FTS mass in SEDT is within the range of decrease observed in the water of the DI controls, and the difference between the normalized 6:2 FTS mass in the SEDT and DI treatments over the incubation period was not significant (Mann-Whitney $U = 17.5$, $p = 0.05$). PFOA and 6:2 FTS had similar mass distributions between the soil and water, with generally 15 % or less of the mass in the soil (Figs. S4 and S5); this outcome was expected based on the similar log D_{ow} values for PFOA (1.58) and 6:2 FTS (1.54) at pH 7 (MarvinSketch, 2018).

Table 2
Percent mass removal for PFOA, 6:2 FTS, and PFOS, and first-order mass removal rate coefficients (k) for PFOS. The removal efficiencies were calculated using the mean total mass from water and soil analyses for days 0 and 45; negative values indicated an increase in mass over time. PFOS (sum L-PFOS and B-PFOS) removal percentages and rates for treatments WSEDT, SEDT, and WSED were adjusted by subtracting the percent removal in the DI treatment. A DI correction was not applied to the PFOA and 6:2 FTS removal rates because removal was less than observed in the DI treatment or an increase in mass over time occurred compared to the DI treatment.

Treatment	PFOA % removal	6:2 FTS % removal	PFOS % removal	L-PFOS % removal	B-PFOS % removal	PFOS k, per day	PFOS $t_{1/2}$, days	PFOS R^2
DI	18.5 ± 8.2	22.2 ± 0.3	2.9 ± 2.6	2.9	2.9	–	–	–
WSEDT	11.0 ± 10.0	−1.9 ± 2.7	46.4 ± 11.0	45.4	49.3	0.0159 ± 0.0052	48.8 ± 16.0	0.986
SEDT	−9.2 ± 5.8	−19.1 ± 1.4	25.5 ± 6.6	25.0	27.1	0.0075 ± 0.0021	100.6 ± 28.0	0.790
WSED	9.2 ± 3.1	−2.3 ± 0.9	11.5 ± 0.9	11.3	12.2	0.0036 ± 0.00022	191.6 ± 11.8	0.436

[k, removal rate coefficient; $t_{1/2}$, half-life; R^2, coefficient of determination].

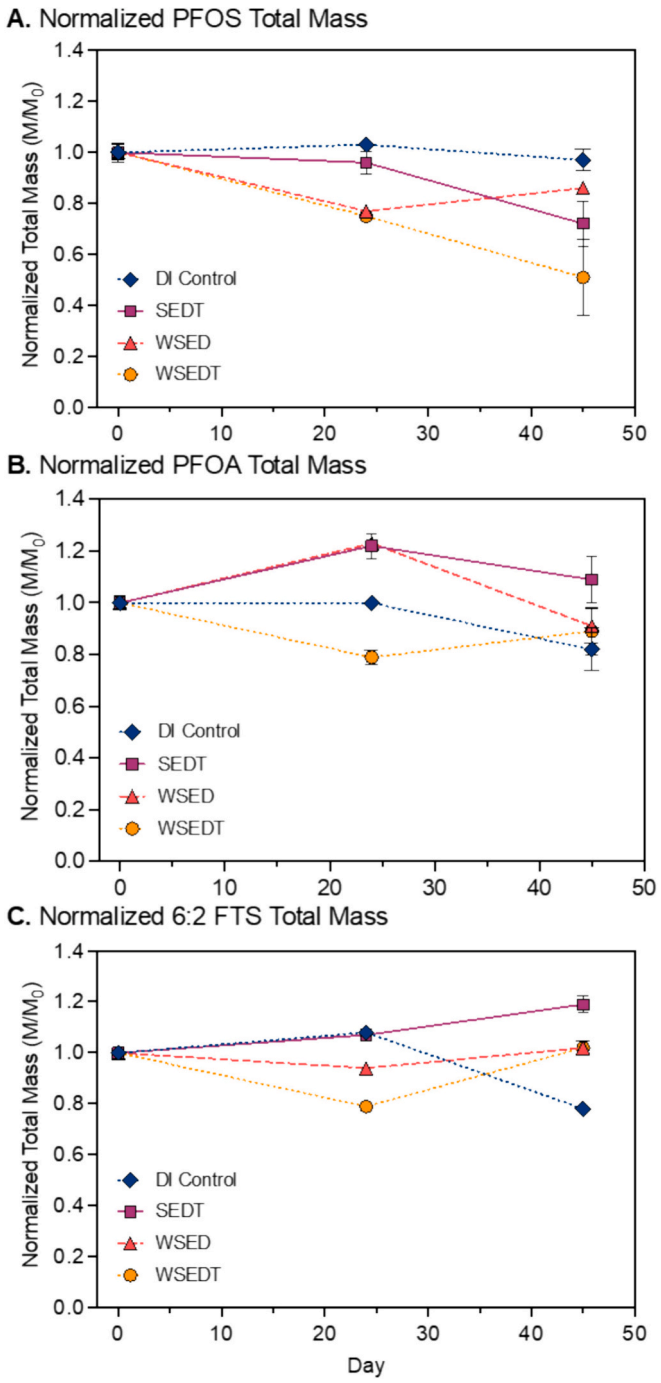

Fig. 3. Change in total mass of (A) PFOS, (B) PFOA, and (C) 6:2 FTS in microcosm samples, calculated from the sum of the mass in the water and the soil at each time point (M) and normalized to the total mass at day 0 (M_0). Error bars show standard deviation of the mean for duplicate bottles; some error bars are too small to be seen.

3.3. Comprehensive PFAS analysis and possible metabolites

For the treatments where PFOS mass reductions were observed, water samples were analyzed to evaluate the sum of PFAS at the beginning and end of the incubation period to evaluate production of potential metabolites (Table S5). The summed concentrations of PFAS and fluorine equivalents in the bioaugmented treatment WSEDT decreased by about 29 % in the water over the 45-day experiment (Table S5). The decrease in total PFAS and fluorine equivalents in WSEDT over time in the full PFAS analysis supports the mass removal of PFOS determined by the targeted analyses of the amended PFAS and shows that the PFOS removal was not balanced by production of PFAA metabolites (Table S5). Sequential reductive defluorination of PFOS could produce shorter chain perfluorinated sulfonates, and concentrations of perfluorohexane sulfonate (PFHxS), perfluoropentane sulfonate (PFPeS), and perfluorobutane sulfonate (PFBS) did increase in the WSEDT water samples over the 45-day incubation period. However, their concentrations were low, with the combined increase in PFHxS, PFPeS, and PFBS concentrations accounting for only 0.22 % of the decrease in PFOS concentrations in the WSEDT microcosm water. Metabolite concentrations measured in other studies with PFOS have also been low. PFBS was reported as a minor PFOS biodegradation product by A6 under anaerobic conditions (Huang and Jaffé, 2019). Perfluorobutanoate (PFBA) was the only other fluorinated intermediate previously identified for anaerobic PFOS biodegradation (Huang and Jaffé, 2019) and was tentatively identified at low concentrations (<2.0 nmoles/L) in the WSEDT and SEDT treatments (Table S5).

The TOP assay results indicated that the PFOS removal in the WSEDT water samples over the 45-day incubation could not be accounted for by production of metabolites that could be converted to PFAAs during the TOP assay, although verification of metabolite production was complicated by the 6:2 FTS also amended to the microcosms (Text S2; Tables S6 and S7). Both the WSEDT and SEDT microcosms showed an increase in perfluorinated carboxylates that could result from 6:2 FTS oxidation during the TOP assay (Weber et al., 2017; Hamid et al., 2020) (Tables S6 and S7). Interestingly, the predominant difference in the post-TOP assay results for the two microcosm treatments was that PFBA concentrations were high for SEDT water samples but were not detected in the WSEDT water samples (Table S6). PFBA is a possible product of 6:2 FTS oxidation but has also been reported as a product of PFOS anaerobic biodegradation (Huang and Jaffé, 2019).

Substantial defluorination of PFOS in the WSEDT treatment was indicated by the combined evidence of significant total mass removal of PFOS documented by water and soil analyses of the microcosms and the low concentrations of metabolites detected in the water by full PFAS analyses. However, the full PFAS analysis did not include measurement of ultrashort-chain PFAS containing less than four carbon atoms. In addition, fluoride analyses were not conducted for this experiment because of relatively high detection limits for fluoride compared to the low fluoride concentrations that could be released from the PFOS concentrations that were amended. The difficulty in measuring fluoride release in biodegradation experiments with environmentally relevant PFAS concentrations has been acknowledged by other researchers (Huang and Jaffé, 2019).

3.4. Biodegradation of cVOCs

To stimulate reductive dehalogenation, cVOCs were added to one treatment with the added WBC-2 culture (WSEDT) and to one treatment that only contained the native microbial community (SEDT). The chlorinated alkane TeCA was added at day 0 at a nominal aqueous-phase concentration of 1000 µg/L (6.0 µmol/L), along with TCE at 100 µg/L (0.76 µmol/L). Reductive dechlorination of TeCA by WBC-2 simultaneously occurs by two pathways — hydrogenolysis to 1,1,2-trichloroethane (112TCA) and 1,2-dichloroethane (12DCA) and dichloroelimination to *cis*- and *trans*-1,2-dichloroethylene (12DCE) with subsequent hydrogenolysis to vinyl chloride (VC) (Lorah et al., 2008; Jones et al., 2006; Lorah et al., 2015; Manchester et al., 2012). Complete dechlorination of these intermediates produces ethene and sometimes ethane. TCE, which can also be produced by abiotic degradation of TeCA, undergoes hydrogenolysis by WBC-2 to 12DCE, VC, and ethene. Methane was detected in microcosm samples from SEDT, WSED, and WSEDT, verifying that the anaerobic conditions needed for complete reductive dehalogenation of the cVOCs occurred in the microcosms (Fig. S9). The methane concentrations were about 1400 µg/L by day 45 in microcosms with and without WBC-2 (Fig. S9).

In the WSEDT treatment, the aqueous-phase concentrations of TeCA and TCE decreased to below detection limits (2.5 µg/L, or 0.015 µmol/L) by day 24 with little accumulation of chlorinated daughter products. The maximum total molar concentration of the chlorinated daughter products in the WSEDT microcosms was more than an order of magnitude lower than the initial TeCA and TCE concentrations (Fig. 4). Soil samples from the WSEDT microcosms also had TeCA concentrations below detection by day 24 (Fig. S8). The low accumulation of chlorinated daughter products indicated that WBC-2 rapidly biodegraded the cVOCs to non-chlorinated end products. Therefore, no inhibition of WBC-2 by the relatively high PFAS concentrations amended to these microcosms was apparent, consistent with a recent study of reductive dechlorination by a different dechlorinating consortium in the presence of PFAA concentrations up to 38.7 mg/L (Hnatko et al., 2023).

In the SEDT treatment, the decrease in TeCA and TCE concentrations with a concomitant increase in chlorinated daughter products indicated reductive dechlorination by the native microbial community (Fig. 4B). However, cVOC removal was incomplete in the SEDT treatment during the 45-day experiment. TeCA concentrations in SEDT were below the detection limit of 0.015 µmol/L by day 45, rather than by day 24 as observed in the WSEDT microcosms, and 12DCA was the dominant daughter product (Fig. 4). 12DCA reached aqueous-phase concentrations of nearly 2.0 µmol/L by day 45 (SEDT, Fig. 4B). Although 12DCE was also produced in SEDT by day 24, continued degradation to VC did not occur.

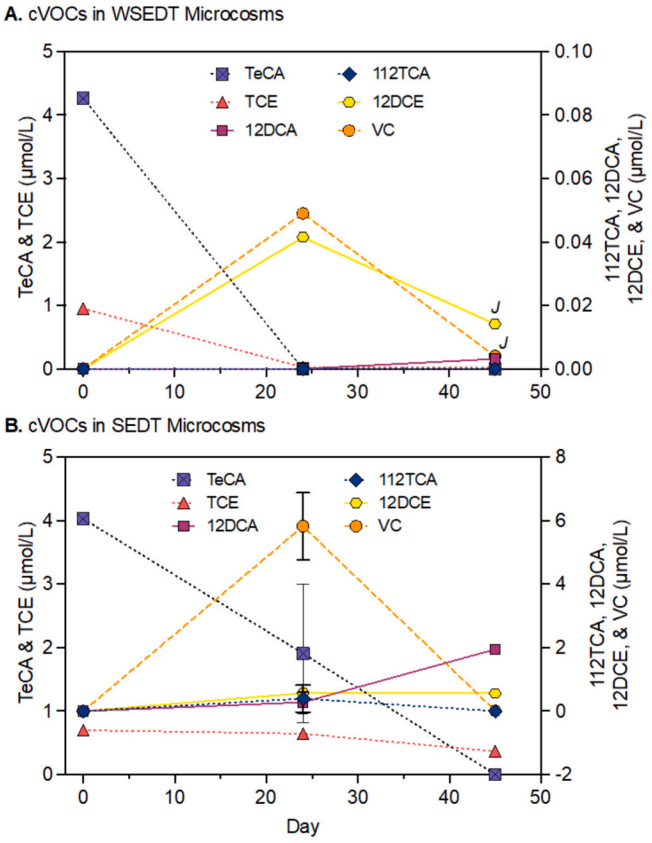

Fig. 4. Molar concentrations of chlorinated volatile organic compounds (cVOCs) measured in water samples from microcosm treatments (A) WSEDT and (B) SEDT, which had 1,1,2,2-tetrachloroethane (TeCA) and trichloroethylene (TCE) added at day 0. Note, the concentration scales for the daughter compounds, 1,1,2-trichloroethane (112TCA), 1,2-dichloroethane (12DCA), 1,2-dichloroethylene (12DCE), and vinyl chloride (VC), differ between the WSEDT and SEDT treatments. Estimated concentrations below the reporting limit are indicated with "*J*". Error bars show standard deviation of the mean for duplicate SEDT bottles; some error bars are too small to be seen.

A link between cVOC degradation and PFOS transformation was inferred by the fact that removal of both contaminants was greatest in the WSEDT microcosms; furthermore, PFOS removal was lowest in the WSED microcosms, which did not contain added cVOCs. Although no known cVOC contamination occurred in the area where the microcosms soil was collected, TCE, 12DCE, and 12DCA were detected in microcosm samples from the two treatments that were not amended with cVOCs, WSED and LC (Fig. S8). Detection of cVOCs was sporadic and low in these treatments but suggested exposure of the native microbial community to halogenated organic contaminants prior to the reported experiments.

3.5. Microbial communities associated with PFOS biodegradation

Microbial community dynamics were assessed in the LC, SED, WSED, and SEDT microcosms at days 0, 24, and 45. NMDS analysis with a Bray-Curtis dissimilarity matrix showed differences in community structure between the different treatments and times (Fig. S10). Permutational multivariate analysis of variance showed that microbial community structure significantly differed by treatment (adonis2, $p = 0.002$, $r^2 = 0.201$) but not by time (adonis2, $p = 0.806$, $r^2 = 0.0817$). The WSEDT samples were most similar to each another and showed shifts along NMDS axis 1 with time. This outcome may be due to the addition of both the WBC-2 consortium and cVOCs to the soil slurry, which provided a known dechlorinating population along with a substrate to support microbial metabolism. Further, the native soil community might not have acclimated to the highly anaerobic conditions and addition of lactate in the microcosms. WSEDT microcosms at day 24 had the highest number of reads and OTUs and the highest diversity based on the Chao1, Shannon, and Inverse Simpson's diversity index (Table S8 and Fig. S11).

Shifts in microbial community structure were supported by differences in the taxonomic composition of the communities in the WSEDT, SEDT, and WSED microcosms (discussed further below, Fig. S12). The WSEDT and WSED treatments had the most phyla detected at >1 % relative abundance, with 12 and 13 different phyla, respectively detected across all sampling times. In contrast, SEDT only had 6 phyla detected at >1 % relative abundance across the time points. The taxonomic composition of replicate microcosms was variable suggesting that the source soil had a high level of microbial heterogeneity.

Firmicutes was the most abundant phylum in all three treatments and the only phylum detected at all time points (Fig. S12). From day 0 to 45, Firmicutes had a significant $\log_2$ fold increase (p-adjusted <0.05, DESeq2 analysis at the phyla-level) in the SEDT microcosms, but no significant $\log_2$ fold change was observed for Firmicutes in the WSEDT or WSED microcosms over the same timeframe. In the WSEDT microcosms, two Firmicutes genera, *Anaeromusa-Anaeroarcus* and *Streptococcus*, had significant $\log_2$ fold increases (p-adjusted <0.05, DESeq2 analysis at the genus-level) from day 0 to 45. Two Firmicutes genera had significant $\log_2$ fold changes in the WSED microcosms: *Sporomusa* decreased while unclassified Clostridiaceae significantly increased from day 0 to 45 (p-adjusted <0.05, DESeq2 analysis at the genus-level). Significant $\log_2$ fold increases were seen from day 0 to 45 for six genera in the SEDT microcosms: unclassified Sporomusaceae; *Ruminiclostridium; Pelosinus; Clostridium sensu stricto* 12; uncultured Firmicutes; and *Desulfosporosinus* (p-adjusted <0.05, DESeq2 analysis at the genus-level).

The Firmicutes phylum includes facultative and strict anaerobic strains, many of which are spore formers and capable of degrading organic contaminants. *Sporomusa* are lactate-fermenting anaerobes, and several strains are known to degrade organic compounds and accumulate acetate (Amano et al., 2018; Sanchez-Andrea et al., 2018; Moe et al., 2012). Possibly, the *Sporomusa*-related OTUs in the WSED microcosms decreased due to competition with other populations in WBC-2 and increased in SEDT due to an increase in native soil OTUs with the addition of lactate. The increase in *Pelosinus* in the SEDT microcosms could be related to the ability of strains in this genus to tolerate or

degrade cVOCs based on previous isolations from chlorinated solvent-contaminated water (Moe et al., 2012). Members of the *Pelosinus* genus are also common in subsurface environments where they are linked to anaerobic metal reduction (Ray et al., 2018).

Desulfosporosinus, a known sulfate-reducer in the Firmicutes phylum, showed the greatest change over time based on relative abundance in the treatments that had the highest PFOS removal, WSEDT and SEDT (Fig. 5A and B, respectively). However, the *Desulfosporosinus* genus only had a significant $\log_2$ fold increase from days 0 to 45 in the SEDT microcosms (Table S8). The lack of significance for *Desulfosporosinus* using DESeq2 in the WSEDT microcosms was likely due to differences in the replicate bottles, which also showed differences in PFOS mass. *Desulfosporosinus* relative abundance also did not significantly change based on DESeq2 in the WSED microcosms. In the WSEDT microcosms, the Campilobacterota genus *Sulfurospirillum*, which includes known sulfate-reducers, also increased in relative abundance. Members of the phylum Campilobacterota markedly increased in relative abundance over time from 0.01 % at day 0 to ~22 % at day 45 in the WSEDT microcosms (Fig. S12). Further, *Sulfurospirillum* strains are known to be able to partially dechlorinate tetrachloroethene and TCE to 12DCE (Fig. 5A). Importantly, this sulfur-reducing genus did not increase in population abundance in the WSED microcosm treatment, which contained the same soil slurry as WSEDT but did not show overall PFOS removal (Table 2).

The Chloroflexi were the second most abundant phyla in the WSEDT and WSED microcosms, but their abundance decreased from day 0 to 45, likely reflecting changes in the WBC-2 community composition during the incubation. However, no significant log2 fold change was observed for Chloroflexi at the phyla-level in the WSEDT or SEDT microcosms from day 0 to 45 (Table S9). Interestingly, Chloroflexi were not detected in the WSED bottles at day 24, but PFOS degradation was observed from day 0 to 24. Chloroflexi increased in relative abundance to above detection at day 45 in the WSED bottles (Fig. S12), resulting in a significant log2 fold increase (p-adjusted >0.05, DESeq2 analysis at the phyla-level, Table S9). At the genus-level for WSED microcosms, a single OTU within the Chloroflexi had a significant log2 fold increase; this OTU was within the candidate phylum Dormibacteraeota (formerly AD3 clade). Candidate phylum Dormibacteraeota has no known cultured representatives to provide information on their potential function but is regularly found in subsurface soil microbiomes and has genetic traits with the potential for life in oligotrophic environments (Brewer et al., 2019). WSEDT had two Chloroflexi OTUs with significant log2 fold changes: the unclassified TK10 clade had a significant log2 fold decrease; and an OTU in the Anaerolineaceae family had a significant log2 fold increase (p-adjusted >0.05, DESeq2 analysis at the genus-level). No significant log2 fold changes were seen for Chloroflexi OTUs in the SEDT treatments. The Chloroflexi phylum includes members of *Dehalococcoides* and *Dehalogenimonas*, two genera in the WBC-2 culture capable of complete dehalorespiration of chlorinated ethenes (Hendrickson et al., 2002; Duhamel and Edwards, 2006; Ewald et al., 2007; Key et al., 2017; Yang et al., 2017; Yang et al., 2020; Chen et al., 2022). Given that WBC-2 was added to both the WSEDT and WSED microcosms, it was surprising that these organisms were minor populations in the microcosms and that neither genus had significant log2 fold changes over time. The complete biodegradation of cVOCs before day 24 in WSED and WSEDT could account for the lack of change in *Dehalococcoides* and *Dehalogenimonas*, but PFOS removal continued in WSEDT through day 45. Thus, the original hypothesis that enhancing reductive dechlorination could also enhance reductive defluorination was not verified by data showing an increase in well-known dehalorespirers. The dehalogenating Chloroflexi were potentially sensitive to the PFAS, but the concentrations amended to the microcosms were well below the 38.7 mg/L threshold reported as inhibitory for another dehalogenating consortium (Hnatko et al., 2023).

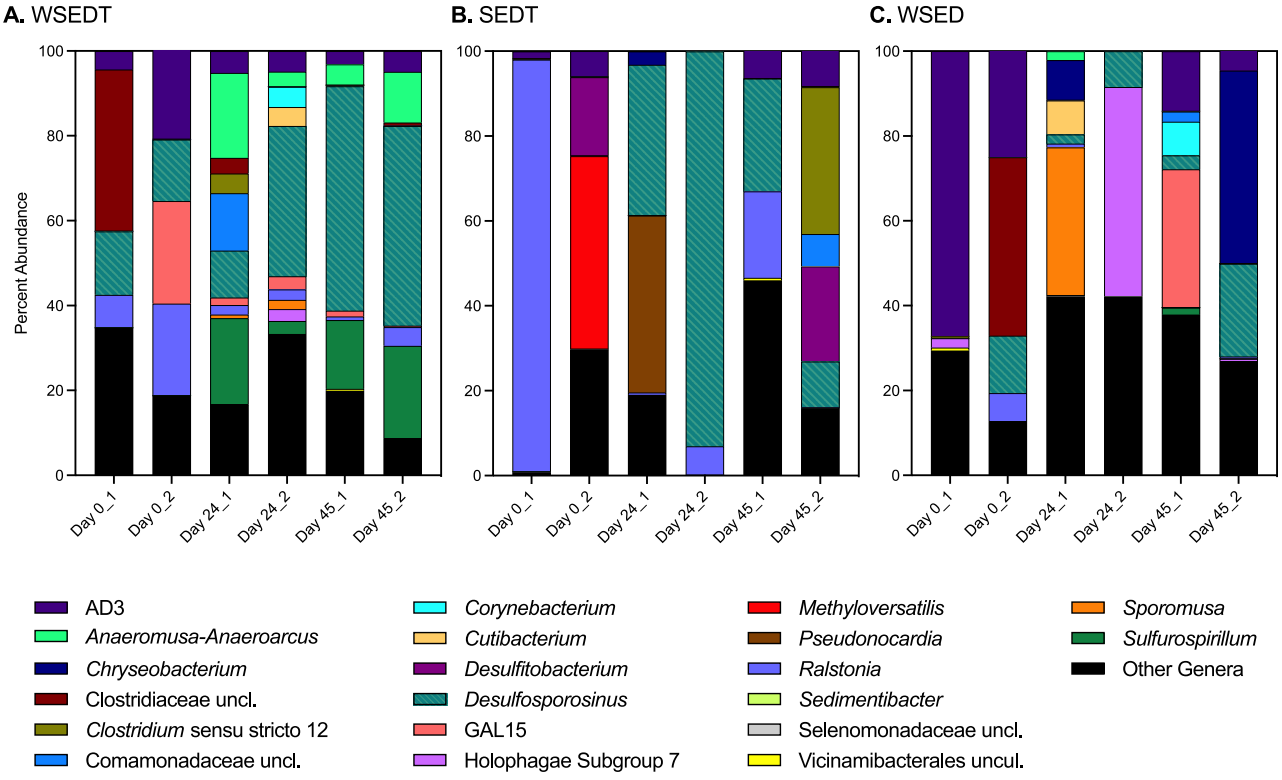

Fig. 5. Microbial community composition at the genus level for populations with >1 % relative abundance in the microcosm treatments (A) WSEDT, (B) SEDT, and (C) WSED. Results are shown for each duplicate microcosm bottle at each time step. Note that sample SEDT Day 0_2 had <5000 reads. The biom file of taxonomic assignment of all operational taxonomic units (OTUs) can be found in Lorah et al. (2024).

4. Conclusions and environmental implications

Despite the voluntary phase-out of PFOS manufacturing in the United States that began in 2000, PFOS remains one of the most frequently detected and most concentrated PFAS in surface water and groundwater near AFFF sites and elsewhere (Zhang et al., 2016; McMahon et al., 2022; East et al., 2021; Johnson et al., 2022). Bioremediation has filled a critical role for *in situ* treatment of chlorinated organic contaminants, and our results have important implications for similar development of *in situ* treatment methods for PFAS and for advancing knowledge of natural attenuation processes (Newell et al., 2021a, 2021b). We showed evidence of reductive biodefluorination with (1) removal rates quantified by PFOS mass balance between the water and soil over time and (2) indication of defluorination to non-fluorinated compounds or ultrashort-chain PFAS by the low or non-detectable concentrations of potential metabolites in the full PFAS analysis and the TOP assay. Furthermore, the association of PFOS degradation with cVOC biodegradation and increased abundance of some microbial populations associated with cVOC biodegradation indicated a biological removal process for PFOS. The lack of removal of 6:2 FTS and PFOA in the same treatments confirmed that the biodegradation pathways were unique to PFOS, a compound that has previously proven difficult to transform through abiotic and biotic processes (Sharifan et al., 2021). Importantly, the PFOS biodegradation reported here was the same for the linear and branched isomers of PFOS (Table 2), whereas abiotic degradation of PFOS typically results in minimal changes to linear isomers compared to branched forms (Patch et al., 2022; Ochoa-Herrera et al., 2008).

The high rate of PFOS biodegradation observed with addition of the WBC-2 anaerobic dehalogenating culture and cVOCs builds on the only other culture, namely enrichments with A6, reported to be capable of reductive biodefluorination of PFOS under environmentally relevant conditions (Huang and Jaffé, 2019; Jaffé et al., 2021; Sima et al., 2023). In a recent study using gamma irradiation to emulate reductive defluorination, PFOS degraded more readily than the short-chain perfluorinated sulfonates, PFHxS and PFBS (Patch et al., 2022). Lower carbon-fluorine (C—F) bond energies have previously been calculated for long-chain PFAS, and Patch et al. (2022) theorized that the rotation of the longer helical chain of PFOS can more readily expose the C—F bond to reactive species. Our results support the conclusion by Patch et al. (2022) that reductive defluorination is the best approach for PFOS treatment, rather than oxidation methods, but we provided additional evidence that such reductive defluorination could be biotically achieved. The overall degradation with gamma irradiation was 61 ± 1 % at pH 7 for 1.9 mg/L PFOS (Patch et al., 2022) compared 46.4 ± 11.0 % PFOS removal with the WBC-2 bioaugmented experiment reported here (Table 2).

The increased abundance of sulfate reducers in the genus *Desulfosporosinus* (Firmicutes) and *Sulfurospirillum* (Campilobacterota) observed with PFOS biodegradation in our experiments was likely linked to the importance of reduction of the sulfur-containing head group to initiate biodegradation by desulfonation, as noted in biodegradation studies with 6:2 FTS and other sulfonates (Yang et al., 2022; Shaw et al., 2019). The important role of anaerobic desulfonation by sulfate reducers, including Firmicutes, has recently been shown for biodegradation of ubiquitous natural organosulfur compounds (Burrichter et al., 2018; Liu et al., 2020). PFOS has often been cited as highly recalcitrant due to the protective nature of the sulfonate head group, but removal of this functional group or breaking a C—F bond greatly increases the susceptibility of the fluorine atoms on the remaining helical carbon chain to reaction (Zhang et al., 2013; Battye et al., 2022). The apparent lack of desulfonation of 6:2 FTS, which is structurally similar to PFOS, in our experiment was surprising, but the lower amended concentration of 6:2 FTS might have limited or obscured 6:2 FTS degradation compared to PFOS.

Sulfate-reducers may play a more direct role in reductive defluorination of PFOS, as they do for other halogenated organics, and therefore warrant additional study. *Desulfosporosinus spp.* were also a component of the microbial community that increased over time in incubations of A6 enrichments with PFOS or PFHxS but not PFOA (Huang and Jaffé, 2019; Jaffé et al., 2021). In addition to the presence of sulfate reducers noted in laboratory experiments with PFAS, a field study in groundwater at a fire-fighting training area found a strong positive correlation between C4-C7 PFAS concentrations and the distribution of sulfate reducers in the genus *Desulfococcus* (Desulfobacterota) (O'Carroll et al., 2020). In another field study at a site with both PFAS and a mixture of cVOCs, including chlorinated methane, ethanes, and TCE and other ethenes, correlations were not observed between PFAS levels and sulfate reducers or known dehalorespirers (Tang et al., 2022). However, denitrifying conditions predominated at this site, and cVOC reductive dechlorination was incomplete.

In anaerobic PFAS biodegradation experiments with the KB-1 dehalogenating culture (Yu et al., 2020), neither an increased abundance of sulfur reducers nor *Dehalococcoides* (Chloroflexi), the primary dehalorespirer in KB-1, was observed. However, those experiments did not include PFOS or other fully saturated sulfonates (Yu et al., 2020). The lack of association between PFAS degradation and known dechlorinating populations in our study with WBC-2 or in the study with KB-1 (Yu et al., 2020) may indicate their lack of involvement in PFAS reductive defluorination. Alternatively, low population abundances could enable reductive defluorination activity. Notably, complete cVOC degradation occurred in the WSEDT treatment by day 24 when the population abundance of known dechlorinating species was low (Fig. S12, Table S9); thus, the involvement of known dechlorinating species in PFOS degradation cannot be ruled out. Other studies have shown that low populations of dehalorespirers, such as *Dehalococcoides* can drive critical reductive dechlorination reactions (Underwood et al., 2022; Clark et al., 2018).

A microbial consortium is likely required to facilitate biodegradation of PFOS and other fluorinated compounds, in a manner similar to the different species that directly or indirectly facilitate reaction steps for chlorinated organic compounds, such as TCE and TeCA (Jones et al., 2006; Manchester et al., 2012; Yan et al., 2016), chlorobenzenes (Kurt and Spain, 2013; Chow et al., 2020), and polychlorinated biphenyls (Payne et al., 2013). The apparent association between degradation of PFOS, a fluorinated alkane, and the chlorinated alkane dechlorination pathway for TeCA that led to accumulation of 12DCA in the SEDT treatment is intriguing. It is possible that addition of WBC-2 and TeCA was successful in stimulating PFOS defluorination, as opposed to the incomplete degradation observed in SEDT, because of the higher populations of species capable of complete degradation of saturated alkanes. WBC-2 is maintained to keep both alkane and alkene dechlorination pathways active and contains a wide diversity of organisms that may harbor unknown dehalogenases (Molenda et al., 2016). Additional testing of the dehalogenating populations in the WBC-2 culture during PFOS degradation, along with identification of potential metabolites and fluoride measurements, could better define degradation pathways. Metabolite identification linked to associated microbial populations is critical for defining degradation pathways and clarifying the apparent preference for PFOS in this study. Future tests could include individual amendments of PFOS and 6:2 FTS at the same molar concentrations. Although addition of cVOCs with WBC-2 appeared to stimulate the greatest PFOS removal in the reported experiments, the fact that PFOS degradation continued long after cVOCs were degraded is promising and suggests that further definition of the microbial populations involved in PFOS degradation will allow development of bioremediation methods without cVOC addition.

Supplementary data to this article can be found online at https://doi.org/10.1016/j.scitotenv.2024.172996.

CRediT authorship contribution statement

Michelle M. Lorah: Writing – review & editing, Writing – original draft, Visualization, Project administration, Funding acquisition, Formal analysis, Conceptualization. **Ke He:** Writing – review & editing, Formal analysis, Data curation. **Lee Blaney:** Writing – review & editing, Formal analysis, Data curation. **Denise M. Akob:** Writing – review & editing, Writing – original draft, Visualization, Formal analysis, Data curation. **Cassandra Harris:** Writing – original draft, Visualization, Investigation, Formal analysis, Data curation. **Andrea Tokranov:** Writing – review & editing, Formal analysis, Data curation. **Zachary Hopkins:** Writing – review & editing, Formal analysis, Data curation. **Brian P. Shedd:** Resources, Funding acquisition.

Declaration of competing interest

The authors declare that they have no known competing financial interests or personal relationships that could have appeared to influence the work reported in this paper.

Data availability

All data and analysis code are available in the Supplemental Information and in a data release (Lorah et al., 2024).

Acknowledgements

This project was supported by the U.S. Geological Survey (USGS) through the Environmental Health Program of the Ecosystem Mission Area and the U.S. Army Corps of Engineers, Baltimore District. We thank Scott Forbes, U.S. Army Corps of Engineers, for assistance collecting field samples. We also thank Carol Morel, currently with the USGS National Climate Adaptation Science Center, for assistance in experiment preparation and sampling.

Any use of trade, firm, or product names is for descriptive purposes only and does not imply endorsement by the U.S. Government. The authors declare no competing financial interest.

References

Amano, N., Yamamuro, A., Miyahara, M., Kouzuma, A., Abe, T., Watanabe, K., 2018. *Methylomusa anaerophila* gen. nov., sp nov., an anaerobic methanol-utilizing bacterium isolated from a microbial fuel cell. Int. J. Syst. Evol. Microbiol. 68, 1118–1122. https://doi.org/10.1099/ijsem.0.002635.

Anderson, R.H., Long, G.C., Porter, R.C., Anderson, J.K., 2016. Occurrence of select perfluoroalkyl substances at U.S. air Force aqueous film-forming foam release sites other than fire-training areas: Field-validation of critical fate and transport properties. Chemosphere 150, 678–685. https://doi.org/10.1016/j.chemosphere.2016.01.014.

Ankley, G.T., Cureton, P., Hoke, R.A., Houde, M., Kumar, A., Kurias, J., Lanno, R., McCarthy, C., Newsted, J., Salice, C.J., Sample, B.E., Sepúlveda, M.S., Steevens, J., Valsecchi, S., 2021. Assessing the ecological risks of per- and polyfluoroalkyl substances: current state-of-the science and a proposed path forward. Environ. Toxicol. Chem. 40, 564–605. https://doi.org/10.1002/etc.4869.

Apprill, A., McNally, S., Parsons, R., Weber, L., 2015. Minor revision to V4 region SSU rRNA 806R gene primer greatly increases detection of SAR11 bacterioplankton. Aquat. Microb. Ecol. 75 (2), 129–137. https://doi.org/10.3354/ame01753.

Battye, N.J., Patch, D.J., Roberts, D.M.D., O'Connor, N.M., Turner, L.P., Kueper, B.H., Hulley, M.E., Weber, K.P., 2022. Use of a horizontal ball mill to remediate per- and polyfluoroalkyl substances in soil. Sci. Total Environ. 835, 155506 https://doi.org/10.1016/j.scitotenv.2022.155506.

Bossert, I.D., Häggblom, M.M., Young, L.Y., 2003. Microbial ecology of dehalogenation. In: Häggblom, Max M., Bossert, Ingeborg D. (Eds.), Dehalogenation: Microbial Processes and Environmental Applications. Springer US, Boston, MA.

Brewer, T.E., Aronson, E.L., Arogyaswamy, K., Billings, S.A., Botthoff, J.K., Campbell, A. N., Dove, N.C., Fairbanks, D., Gallery, R.E., Hart, S.C., Kaye, J., King, G., Logan, G., Lohse, K.A., Maltz, M.R., Mayorga, E., O'Neill, C., Owens, S.M., Packman, A., Pett-Ridge, J., Plante, A.F., Richter, D.D., Silver, W.L., Yang, W.H., Fierer, N., 2019. Ecological and genomic attributes of novel bacterial taxa that thrive in subsurface soil horizons. mBio 10. https://doi.org/10.1128/mbio.01318-19, 10.1128/mbio.01318-19.

Buck, R.C., Franklin, J., Berger, U., Conder, J.M., Cousins, I.T., De Voogt, P., Jensen, A. A., Kannan, K., Mabury, S.A., Van Leeuwen, S.P., 2011. Perfluoroalkyl and polyfluoroalkyl substances in the environment: terminology, classification, and origins. Integr. Environ. Assess. Manag. 7, 513–541. https://doi.org/10.1002/ieam.258.

Burrichter, A., Denger, K., Franchini, P., Huhn, T., Müller, N., Spiteller, D., Schleheck, D., 2018. Anaerobic degradation of the plant sugar sulfoquinovose concomitant with H_2S production: *Escherichia coli* K-12 and *Desulfovibrio* sp. strain DF1 as co-culture model. Front. Microbiol. 9, 2792. https://doi.org/10.3389/fmicb.2018.02792.

Caporaso, J.G., Lauber, C.L., Walters, W.A., Berg-Lyons, D., Huntley, J., Fierer, N., Owens, S.M., Betley, J., Fraser, L., Bauer, M., Gormley, N., Gilbert, J.A., Smith, G., Knight, R., 2012. Ultra-high-throughput microbial community analysis on the Illumina HiSeq and MiSeq platforms. ISME J. 6 (8), 1621–1624. https://doi.org/10.1038/ismej.2012.8.

Chen, G., Kara Murdoch, F., Xie, Y., Murdoch, R.W., Cui, Y., Yang, Y., Yan, J., Key, T.A., Loffler, F.E., 2022. Dehalogenation of chlorinated ethenes to ethene by a novel isolate, "*Candidatus* Dehalogenimonas etheniformans". Appl. Environ. Microbiol. 88 (12), e0044322 https://doi.org/10.1128/aem.00443-22.

Chow, S.J., Lorah, M.M., Wadhawan, A.R., Durant, N.D., Bouwer, E.J., 2020. Sequential biodegradation of 1,2,4-trichlorobenzene at oxic-anoxic groundwater interfaces in model laboratory columns. J. Contam. Hydrol. 231, 103639 https://doi.org/10.1016/j.jconhyd.2020.103639.

Clark, K., Taggart, D.M., Baldwin, B.R., Ritalahti, K.M., Murdoch, R.W., Hatt, J.K., Löffler, F.E., 2018. Normalized quantitative PCR measurements as predictors for ethene formation at sites impacted with chlorinated ethenes. Environ. Sci. Technol. 52 (22), 13410–13420. https://doi.org/10.1021/acs.est.8b04373.

Duhamel, M., Edwards, E.A., 2006. Microbial composition of chlorinated ethene-degrading cultures dominated by *Dehalococcoides*. FEMS Microbiol. Ecol. 58 (3), 538–549. https://doi.org/10.1111/j.1574-6941.2006.00191.x.

East, A., Anderson, R.H., Salice, C.J., 2021. Per- and polyfluoroalkyl substances (PFAS) in surface water near US Air Force bases: prioritizing individual chemicals and mixtures for toxicity testing and risk assessment. Environ. Toxicol. Chem. 40, 859–870. https://doi.org/10.1002/etc.4893.

Ewald, E.-M., Wagner, A., Nijenhuis, I., Richnow, H.-H., Lechner, U., 2007. Microbial dehalogenation of trichlorinated dibenzo-p-dioxins by a *Dehalococcoides*-containing mixed culture is coupled to carbon isotope fractionation. Environ. Sci. Technol. 41 (22), 7744–7751. https://doi.org/10.1021/es070935g.

Fitzgerald, N.J.M., Wargenau, A., Sorenson, C., Pedersen, J., Tufenkji, N., Novak, P.J., Simcik, M.F., 2018. Partitioning and accumulation of perfluoroalkyl substances in model lipid bilayers and bacteria. Environ. Sci. Technol. 52, 10433–10440. https://doi.org/10.1021/acs.est.8b02912.

Glüge, J., Scheringer, M., Cousins, I.T., DeWitt, J.C., Goldenman, G., Herzke, D., Lohmann, R., Ng, C.A., Trier, X., Wang, Z., 2020. An overview of the uses of per- and polyfluoroalkyl substances (PFAS). Environ Sci Process Impacts 22, 2345–2373. https://doi.org/10.1039/d0em00291g.

Hamid, H., Li, L.Y., Grace, J.R., 2020. Formation of perfluorocarboxylic acids from 6:2 fluorotelomer sulfonate (6:2 FTS) in landfill leachate: Role of microbial communities. Environ. Pollut. 259, 113835. https://doi.org/10.1016/j.envpol.2019.113835.

Harding-Marjanovic, K.C., Houtz, E.F., Yi, S., Field, J.A., Sedlak, D.L., Alvarez-Cohen, L., 2015. Aerobic biotransformation of fluorotelomer thioether amido sulfonate (Lodyne) in AFFF-amended microcosms. Environ. Sci. Technol. 49, 7666–7674. https://doi.org/10.1021/acs.est.5b01219.

Hendrickson, E.R., Payne, J.A., Young, R.M., Starr, M.G., Perry, M.P., Fahnestock, S., Ellis, D.E., Ebersole, R.C., 2002. Molecular analysis of *Dehalococcoides* 16S ribosomal DNA from chloroethene-contaminated sites throughout North America and Europe. Appl. Environ. Microbiol. 68 (2), 485–495. https://doi.org/10.1128/AEM.68.2.485-495.2002.

Hnatko, J.P., Liu, C., Elsey, J.L., Dong, S., Fortner, J.D., Pennell, K.D., Abriola, L.M., Cápiro, N.L., 2023. Microbial reductive dechlorination by a commercially available dechlorinating consortium is not inhibited by perfluoroalkyl acids (PFAAs) at field-relevant concentrations. Environ. Sci. Technol. 57, 8301–8312. https://doi.org/10.1021/acs.est.2c04815.

Huang, S., Jaffé, P.R., 2018. Isolation and characterization of an ammonium-oxidizing iron reducer: acidimicrobiaceae sp. A6. PloS One 13 (4), e0194007. https://doi.org/10.1371/journal.pone.0194007.

Huang, S., Jaffé, P.R., 2019. Defluorination of perfluorooctanoic acid (PFOA) and perfluorooctane sulfonate (PFOS) by *Acidimicrobium* sp. strain A6. Environ. Sci. Technol. 53, 11410–11419. https://doi.org/10.1021/acs.est.9b04047.

Huang, S., Chen, C., Peng, X., Jaffé, P.R., 2016. Environmental factors affecting the presence of Acidimicrobiaceae and ammonium removal under iron-reducing conditions in soil environments. Soil Biol. Biochem. 98, 148–158. https://doi.org/10.1016/j.soilbio.2016.04.012.

Huang, S., Sima, M., Long, Y., Messenger, C., Jaffé, P.R., 2022. Anaerobic degradation of perfluorooctanoic acid (PFOA) in biosolids by *Acidimicrobium* sp. strain A6. J. Hazard. Mater. 424, 127699 https://doi.org/10.1016/j.jhazmat.2021.127699.

Jaffé, P.R., Huang, S., Sima, M., Ross, I., Liu, J., 2021. ER20–1219: biotransformation and potential mineralization of PFOS, PFHxS, and PFOA by Acidimicrobiaceae sp. In: A6 under iron Reducing Conditions. SERDP Final Report. https://serdp-estcp.org/index.php//content/download/53927/529646/file/ER20-1219%20Final%20Report.pdf.

Johnson, G.R., Brusseau, M.L., Carroll, K.C., Tick, G.R., Duncan, C.M., 2022. Global distributions, source-type dependencies, and concentration ranges of per- and polyfluoroalkyl substances in groundwater. Sci. Total Environ. 841, 156602 https://doi.org/10.1016/j.scitotenv.2022.156602.

Jones, E.J.P., Voytek, M.A., Lorah, M.M., Kirshtein, J.D., 2006. Characterization of a microbial consortium capable of rapid and simultaneous dechlorination of 1,1,2,2-tetrachloroethane and chlorinated ethane and ethene intermediates. Biorem. J. 10, 153–168. https://doi.org/10.1080/10889860601021399.

Key, T.A., Bowman, K.S., Lee, I., Chun, J., Albuquerque, L., da Costa, M.S., Rainey, F.A., Moe, W.M., 2017. *Dehalogenimonas formicexedens* sp. nov., a chlorinated alkane-respiring bacterium isolated from contaminated groundwater. Int. J. Syst. Evol. Microbiol. 67 (5), 1366–1373. https://doi.org/10.1099/ijsem.0.001819.

Kozich, J.J., Westcott, S.L., Baxter, N.T., Highlander, S.K., Schloss, P.D., 2013. Development of a dual-index sequencing strategy and curation pipeline for analyzing amplicon sequence data on the MiSeq Illumina sequencing platform. Appl. Environ. Microbiol. 79 (17), 5112–5120. https://doi.org/10.1128/AEM.01043-13.

Kucharzyk, K.H., Darlington, R., Benotti, M., Deeb, R., Hawley, E., 2017. Novel treatment technologies for PFAS compounds: a critical review. J. Environ. Manage. 204, 757–764. https://doi.org/10.1016/j.jenvman.2017.08.016.

Kurt, Z., Spain, J.C., 2013. Biodegradation of chlorobenzene, 1,2-dichlorobenzene, and 1,4-dichlorobenzene in the vadose zone. Environ. Sci. Technol. 47, 6846–6854. https://doi.org/10.1021/es3049465.

Liu, J., Wei, Y., Lin, L., Teng, L., Yin, J., Lu, Q., Chen, J., Zheng, Y., Li, Y., Xu, R., Zhai, W., Liu, Y., Liu, Y., Cao, P., Ang, E.L., Zhao, H., Yuchi, Z., Zhang, Y., 2020. Two radical-dependent mechanisms for anaerobic degradation of the globally abundant organosulfur compound dihydroxypropanesulfonate. Proc. Natl. Acad. Sci. USA 117 (27), 15599–15608. https://doi.org/10.1073/pnas.2003434117.

Lorah, M.M., Majcher, E.H., Jones, E.J.P., Voytek, M.A., 2008. Microbial consortia development and microcosm and column experiments for enhanced bioremediation of chlorinated volatile organic compounds, West Branch Canal Creek wetland area, Aberdeen Proving Ground, Maryland. US Geol. Surv. Sci. Investig. Rep. 2007–5165 https://doi.org/10.3133/sir20075165, 79 p. SIR 2007-5165_508.pdf (usgs.gov).

Lorah, M.M., Walker, C., Graves, D., 2015. Performance of an anaerobic, static bed, fixed film bioreactor for chlorinated solvent treatment. Biodegradation 26, 1–17. https://doi.org/10.1007/s10532-015-9738-1.

Lorah, M.M., Baesman, S.M., He, K., Blaney, L., Akob, D.M., Harris, C.R., Tokranov, A.K., Hopkins, Z.R., 2024. Per- and Polyfluoroalkyl Substances (PFAS) and Volatile Organic Compounds Measured in Laboratory Microcosm Experiments with Soil from Fort Drum. U.S. Geological Survey Data Release, New York. https://doi.org/10.5066/P9VJ6HY8.

Love, M.I., Huber, W., Anders, S., 2014. Moderated estimation of fold change and dispersion for RNA-seq data with DESeq2. Genome Biol. 15, 550. https://doi.org/10.1186/s13059-014-0550-8.

Majcher, E.H., Phelan, D.J., Lorah, M.L., McGinty, A.L., 2007. Characterization of preferential ground-water seepage from a chlorinated hydrocarbon-contaminated aquifer to West Branch Canal Creek, Aberdeen Proving Ground, Maryland. In: U.S. Geological Survey Scientific Investigations Report 2006–5233. https://doi.org/10.3133/sir20065233. http://md.water.usgs.gov/publications.

Manchester, M.J., Hug, L.A., Zarek, M., Zila, A., Edwards, E.A., 2012. Discovery of a trans-dichloroethene-respiring *Dehalogenimonas* species in the 1,1,2,2-tetrachloroethane-dechlorinating WBC-2 consortium. Appl. Environ. Microbiol. 78, 5280–5287.

MarvinSketch, 2018. Marvin 18.24.0, 2018, ChemAxon. http://www.chemaxon.com.

McMahon, P.B., Tokranov, A.K., Bexfield, L.M., Lindsey, B.D., Johnson, T.D., Lombard, M.A., Watson, E., 2022. Perfluoroalkyl and polyfluoroalkyl substances in groundwater used as a source of drinking water in the eastern United States. Environ. Sci. Technol. 56, 2279–2288. https://doi.org/10.1021/acs.est.1c04795.

McMurdie, P.J., Holmes, S., 2013. phyloseq: an R package for reproducible interactive analysis and graphics of microbiome census data. PloS One 8, e61217. https://doi.org/10.1371/journal.pone.0061217.

Moe, W.M., Stebbing, R.E., Rao, J.U., Bowman, K.S., Nobre, M.F., da Costa, M.S., Rainey, F.A., 2012. *Pelosinus defluvii* sp. nov., isolated from chlorinated solvent-contaminated groundwater, emended description of the genus *Pelosinus* and transfer of *Sporotalea propionica* to *Pelosinus propionicus* comb. nov. Int. J. Syst. Evol. Microbiol. 62 (6), 1369–1376. https://doi.org/10.1099/ijs.0.033753-0.

Molenda, O., Quaile, A.T., Edwards, E.A., 2016. *Dehalogenimonas* sp. strain WBC-2 genome and identification of its trans-dichloroethene reductive dehalogenase, TdrA. Appl. Environ. Microbiol. 82, 40–50. https://doi.org/10.1128/AEM.02017-15.

Mumford, A.C., Maloney, K.O., Akob, D.M., Nettemann, S., Proctor, A., Ditty, J., Ulsamer, L., Lookenbill, J., Cozzarelli, I.M., 2020. Shale gas development has limited effects on stream biology and geochemistry in a gradient-based, multiparameter study in Pennsylvania. Proc. Natl. Acad. Sci. 117 (7), 3670–3677. https://doi.org/10.1073/pnas.1911458117.

Munoz, G., Fechner, L.C., Geneste, E., Pardon, P., Budzinski, H., Labadie, P., 2018. Spatio-temporal dynamics of per and polyfluoroalkyl substances (PFASs) and transfer to periphytic biofilm in an urban river: case-study on the River Seine. Environ. Sci. Pollut. Res. 25, 23574–23582. https://doi.org/10.1007/s11356-016-8051-9.

Newell, C.J., Adamson, D.T., Poonam, R.K., Blossom, N.N., Connor, J.A., Popovic, J., Stroo, H.F., 2021a. Monitored natural attenuation to manage PFAS impacts to groundwater: potential guidelines. Remediat. J. 31 (4), 7–17. https://doi.org/10.1002/rem.21697.

Newell, C.J., Adamson, D.T., Poonam, R.K., Blossom, N.N., Connor, J.A., Popovic, J., Stroo, H.F., 2021b. Monitored natural attenuation to manage PFAS impacts to groundwater: scientific basis. Groundw. Monit. Remediat. 41 (4), 76–89. https://doi.org/10.1111/gwmr.12486.

O'Carroll, Denis M., Jeffries, Thomas C., Lee, Matthew J., Le, Song Thao, Yeung, Anna, Wallace, Sarah, Battye, Nick, Patch, David J., Manefield, Michael J., Weber, Kela P., 2020. Developing a roadmap to determine per- and polyfluoroalkyl substances-microbial population interactions. Sci. Total Environ. 712, 135994 https://doi.org/10.1016/j.scitotenv.2019.135994.

Ochoa-Herrera, V., Sierra-Alvarez, R., Somogyi, A., Jacobsen, N.E., Wysocki, V.H., Field, J.A., 2008. Reductive defluorination of perfluorooctane sulfonate. Environ. Sci. Technol. 42 (9), 3260–3264. https://doi.org/10.1021/es702842q.

Ochoa-Herrera, V., Field, J.A., Luna-Velasco, A., Sierra-Alvarez, R., 2016. Microbial toxicity and biodegradability of perfluorooctane sulfonate (PFOS) and shorter chain perfluoroalkyl and polyfluoroalkyl substances (PFASs). Environ. Sci.: Processes Impacts 18, 1236–1246. https://doi.org/10.1039/c6em00366d.

Oksanen, J., Blanchet, F.G., Kindt, R., Legendre, P., Minchin, P.R., O'Hara, R.B., Simpson, G.L., Solymos, P., Stevens, M.H.H., Szoecs, E., Wagner, H., 2018. vegan: community ecology package. R package version 2.5-1, vR package version 2.5-1. https://cran.r-project.org/web/packages/vegan/.

Oksanen, J., Blanchet, F.G., Friendly, M., Kindt, R., Legendre, P., McGlinn, D., Minchin, P.R., O'Hara, R.B., Simpson, G.L., Solymos, P., Stevens, M.H.H., Szoecs, E., Wagner, H., 2019. vegan: community ecology package (Vers. 2.5-5), v2.5-5. https://CRAN.R-project.org/package=vegan.

Parada, A.E., Needham, D.M., Fuhrman, J.A., 2016. Every base matters: assessing small subunit rRNA primers for marine microbiomes with mock communities, time series and global field samples. Environ. Microbiol. 18 (5), 1403–1414. https://doi.org/10.1111/1462-2920.13023.

Park, S., Lee, L.S., Medina, V.F., Zull, A., Waisner, S., 2016. Heat-activated persulfate oxidation of PFOA, 6:2 fluorotelomer sulfonate, and PFOS under conditions suitable for in-situ groundwater remediation. Chemosphere 145, 376–383. https://doi.org/10.1016/j.chemosphere.2015.11.097.

Park, S., de Perre, C., Lee, L.S., 2017. Alternate reductants with VB12 to transform C8 and C6 perfluoroalkyl sulfonates: limitations and insights into isomer-specific transformation rates, products and pathways. Environ. Sci. Technol. 51, 13869–13877. https://doi.org/10.1021/acs.est.7b03744.

Park, S., Zenobio, J.E., Lee, L.S., 2018. Perfluorooctane sulfonate (PFOS) removal with Pd0/nFe0 nanoparticles: adsorption or aqueous Fe-complexation, not transformation? J. Hazard. Mater. 342, 20–28. https://doi.org/10.1016/j.jhazmat.2017.08.001.

Parsons, J.R., Sáez, M., Dolfing, J., de Voogt, P., 2008. Biodegradation of perfluorinated compounds. In: Whitacre, D.M. (Ed.), Reviews of Environmental Contamination and Toxicology, vol. 196. Springer US, New York, NY.

Patch, D., O'Connor, N., Koch, I., Cresswell, T., Hughes, C., Davies, J.B., Scott, J., O'Carroll, D., Weber, K., 2022. Elucidating degradation mechanisms for a range of per- and polyfluoroalkyl substances (PFAS) via controlled irradiation studies. Sci. Total Environ. 832, 154941 https://doi.org/10.1016/j.scitotenv.2022.154941.

Payne, R.B., Fagervold, S.K., May, H.D., Sowers, K.R., 2013. Remediation of polychlorinated biphenyl impacted sediment by concurrent bioaugmentation with anaerobic halorespiring and aerobic degrading bacteria. Environ. Sci. Technol. 47, 3807–3815. https://doi.org/10.1021/es304372t.

Quast, C., Pruesse, E., Yilmaz, P., Gerken, J., Schweer, T., Yarza, P., Peplies, J., Glockner, F.O., 2013. The SILVA ribosomal RNA gene database project: improved data processing and web-based tools. Nucleic Acids Res. 41, D590–D596. https://doi.org/10.1093/nar/gks1219.

R Core Team, 2015. R: A Language and Environment for Statistical Computing. R Foundation for Statistical Computing, Vienna, Austria. https://www.R-project.org/.

Ray, A.E., Connon, S.A., Neal, A.L., Fujita, Y., Cummings, D.E., Ingram, J.C., Magnuson, T.S., 2018. Metal transformation by a novel *Pelosinus* isolate from a subsurface environment. Front. Microbiol. 9, 1689. https://doi.org/10.3389/fmicb.2018.01689.

Rogers, R.D., Reh, C.M., Breysse, P., 2021. Advancing per- and polyfluoroalkyl substances (PFAS) research: an overview of ATSDR and NCEH activities and recommendations. J. Expo. Sci. Environ. Epidemiol. 31 (6), 961–971. https://doi.org/10.1038/s41370-021-00316-6.

Sanchez-Andrea, I., Florentino, A.P., Semerel, J., Strepis, N., Sousa, D.Z., Stams, A.J.M., 2018. Co-culture of a novel fermentative bacterium, *Lucifera butyrica* gen. nov. sp. nov., with the sulfur reducer *Desulfurella amilsii* for enhanced sulfidogenesis. Front. Microbiol. 9, 3108. https://doi.org/10.3389/fmicb.2018.03108.

Schaefer, C.E., Choyke, S., Ferguson, P.L., Andaya, C., Burant, A., Maizel, A., Strathmann, T.J., Higgins, C.P., 2018. Electrochemical transformations of perfluoroalkyl acid (PFAA) precursors and PFAAs in groundwater impacted with aqueous film forming foams. Environ. Sci. Technol. 52, 10689–10697. https://doi.org/10.1021/acs.est.8b02726.

Schloss, P.D., 2021. MiSeq SOP [Online]. Available: https://mothur.org/wiki/miseq_sop/. (Accessed 3 December 2021).

Schloss, P.D., Westcott, S.L., Ryabin, T., Hall, J.R., Hartmann, M., Hollister, E.B., Lesniewski, R.A., Oakley, B.B., Parks, D.H., Robinson, C.J., Sahl, J.W., 2009. Introducing mothur: open-source, platform-independent, community-supported software for describing and comparing microbial communities. Appl. Environ. Microbiol. 75 (23), 7537–7541. https://doi.org/10.1128/AEM.01541-09.

Sharifan, H., Bagheri, M., Wang, D., Burken, J.G., Higgins, C.P., Liang, Y., Liu, J., Schaefer, C.E., Blotevogel, J., 2021. Fate and transport of per- and polyfluoroalkyl substances (PFASs) in the vadose zone. Sci. Total Environ. 771, 145427 https://doi.org/10.1016/j.scitotenv.2021.145427.

Shaw, D.M.J., Munoz, G., Bottos, E.M., Vo Duy, S., Sauvé, S., Liu, J., Van Hamme, J.D., 2019. Degradation and defluorination of 6:2 fluorotelomer sulfonamidoalkyl betaine and 6:2 fluorotelomer sulfonate by *Gordonia* sp. strain NB4-1Y under sulfur-limiting conditions. Sci. Total Environ. 647, 690–698. https://doi.org/10.1016/j.scitotenv.2018.08.012.

Sima, M.W., Huang, S., Jaffé, P.R., 2023. Modeling the kinetics of perfluorooctanoic and perfluorooctane sulfonic acid biodegradation by *Acidimicrobium* sp. Strain A6 during the feammox process. J. Hazard. Mater. 448, 130903 https://doi.org/10.1016/j.jhazmat.2023.130903.

Sunderland, E.M., Hu, X.C., Dassuncao, C., Tokranov, A.K., Wagner, C.C., Allen, J.G., 2019. A review of the pathways of human exposure to poly- and perfluoroalkyl substances (PFASs) and present understanding of health effects. J. Expo. Sci. Environ. Epidemiol. 29, 131–147. https://doi.org/10.1038/s41370-018-0094-1.

Tang, Z., Song, X., Xu, M., Yao, J., Ali, M., Wang, Q., Zeng, J., Ding, X., Wang, C., Zhang, Z., Liu, X., 2022. Effects of co-occurrence of PFASs and chlorinated aliphatic hydrocarbons on microbial communities in groundwater: a field study. J. Hazard. Mater. 435, 128969 https://doi.org/10.1016/j.jhazmat.2022.128969.

Underwood, J.C., Akob, D.M., Lorah, M.M., Imbrigiotta, T.E., Harvey, R.W., Tiedeman, C.R., 2022. Microbial community response to a bioaugmentation test to degrade trichloroethylene in a fractured rock aquifer, Trenton, N.J. FEMS Microbiol. Ecol. 98 (7), fiac077 https://doi.org/10.1093/femsec/fiac077.

USEPA, 2024. (April 10). PFAS national primary drinking water Regulation. Retrieved from FACT SHEET. epa.gov. (Accessed 26 April 2024).

Walters, W., Hyde, E.R., Berg-Lyons, D., Ackermann, G., Humphrey, G., Parada, A., Gilbert, J.A., Jansson, J.K., Caporaso, J.G., Fuhrman, J.A., Apprill, A., Knight, R., 2016. Improved bacterial 16S rRNA gene (V4 and V4-5) and fungal internal transcribed spacer marker gene primers for microbial community surveys. mSystems 1 (1). https://doi.org/10.1128/mSystems.00009-15.

Wang, Z., Cousins, I.T., Scheringer, M., Hungerbuehler, K., 2015. Hazard assessment of fluorinated alternatives to long-chain perfluoroalkyl acids (PFAAs) and their precursors: status quo, ongoing challenges and possible solutions. Environ. Int. 75, 172–179. https://doi.org/10.1016/j.envint.2014.11.013.

Weber, A.K., Barber, L.B., LeBlanc, D.R., Sunderland, E.M., Vecitis, C.D., 2017. Geochemical and hydrologic factors controlling subsurface transport of poly- and perfluoroalkyl substances, Cape Cod, Massachusetts. Environ. Sci. Technol. 51, 4269–4279. https://doi.org/10.1021/acs.est.6b05573.

Yan, J., Şimşir, B., Farmer, A.T., Bi, M., Yang, Y., Campagna, S.R., Löffler, F.E., 2016. The corrinoid cofactor of reductive dehalogenases affects dechlorination rates and extents in organohalide-respiring *Dehalococcoides mccartyi*. ISME J. 10, 1092–1101. https://doi.org/10.1038/ismej.2015.197.

Yang, Y., Higgins, S.A., Yan, J., Simsir, B., Chourey, K., Iyer, R., Hettich, R.L., Baldwin, B., Ogles, D.M., Loffler, F.E., 2017. Grape pomace compost harbors organohalide-respiring Dehalogenimonas species with novel reductive dehalogenase genes. ISME J. 11 (12), 2767–2780. https://doi.org/10.1038/ismej.2017.127.

Yang, Y., Sanford, R., Yan, J., Chen, G., Capiro, N.L., Li, X., Loffler, F.E., 2020. Roles of organohalide-respiring *Dehalococcoidia* in carbon cycling. mSystems 5 (3). https://doi.org/10.1128/mSystems.00757-19.

Yang, S.-H., Shi, Y., Strynar, M., Chu, K.-H., 2022. Desulfonation and defluorination of 6:2 fluorotelomer sulfonic acid (6:2 FTSA) by *Rhodococcus jostii* RHA1: carbon and sulfur sources, enzymes, and pathways. J. Hazard. Mater. 423, 127052 https://doi.org/10.1016/j.jhazmat.2021.127052.

Yilmaz, P., Parfrey, L.W., Yarza, P., Gerken, J., Pruesse, E., Quast, C., Schweer, T., Peplies, J., Ludwig, W., Glockner, F.O., 2014. The SILVA and "all-species living tree project (LTP)" taxonomic frameworks. Nucleic Acid Res. 42, D643–D648. https://doi.org/10.1093/nar/gkt1209.

Yu, Y., Zhang, K., Li, Z., Ren, C., Chen, J., Lin, Y.-H., Liu, J., Men, Y., 2020. Microbial cleavage of C–F bonds in two C6 per- and polyfluorinated compounds via reductive defluorination. Environ. Sci. Technol. 54, 14393–14402. https://doi.org/10.1021/acs.est.0c04483.

Yu, Y., Che, S., Ren, C., Jin, B., Tian, Z., Liu, J., Men, Y., 2022. Microbial defluorination of unsaturated per- and polyfluorinated carboxylic acids under anaerobic and aerobic conditions: a structure specificity study. Environ. Sci. Technol. 56, 4894–4904. https://doi.org/10.1021/acs.est.1c05509.

Zhang, K., Huang, J., Yu, G., Zhang, Q., Deng, S., Wang, B., 2013. Destruction of perfluorooctane sulfonate (PFOS) and perfluorooctanoic acid (PFOA) by ball milling. Environ. Sci. Technol. 47, 6471–6477. https://doi.org/10.1021/acs.est.1c05509.

Zhang, X., Lohmann, R., Dassuncao, C., Hu, X.C., Weber, A.K., Vecitis, C.D., Sunderland, E.M., 2016. Source attribution of poly- and perfluoroalkyl substances (PFASs) in surface waters from Rhode Island and the New York Metropolitan Area. Environ. Sci. Technol. Lett. 3, 316–321. https://doi.org/10.1021/acs.estlett.6b00255.

Zhang, W., Pang, S., Lin, Z., Mishra, S., Bhatt, P., Chen, S., 2021. Biotransformation of perfluoroalkyl acid precursors from various environmental systems: advances and perspectives. Environ. Pollut. 272, 115908 https://doi.org/10.1016/j.envpol.2020.115908.